DOI:
10.1016/j.joca.2017.08.006
10.1016/j.joca.2017.08.006

Document Version
Peer reviewed version

Accepted Manuscript

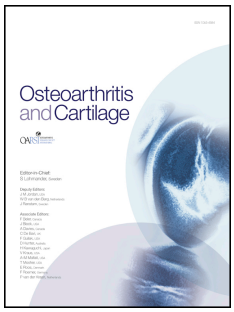

Role of TrkA signalling and mast cells in the initiation of osteoarthritis pain in the monoiodoacetate model

João Sousa-Valente, Laura Calvo, Valentina Vacca, Raffaele Simeoli, Juan Carlos Arévalo, Marzia Malcangio

PII: S1063-4584(17)31149-4

DOI: 10.1016/j.joca.2017.08.006

Reference: YJOCA 4069

To appear in: *Osteoarthritis and Cartilage*

Received Date: 18 April 2017

Revised Date: 10 August 2017

Accepted Date: 17 August 2017

Please cite this article as: Sousa-Valente J, Calvo L, Vacca V, Simeoli R, Arévalo JC, Malcangio M, Role of TrkA signalling and mast cells in the initiation of osteoarthritis pain in the monoiodoacetate model, *Osteoarthritis and Cartilage* (2017), doi: 10.1016/j.joca.2017.08.006.

Role of TrkA signalling and mast cells in the initiation of osteoarthritis pain in the monoiodoacetate model

João Sousa-Valente (JSV)[1], joao.de_sousa_valente@kcl.ac.uk

Laura Calvo (LC)[2, 3], lau@usal.es

Valentina Vacca (VV)[1, 4], valentina.vacca@ibcn.cnr.it

Raffaele Simeoli (RS)[1], raffaele.simeoli@kcl.ac.uk

Juan Carlos Arévalo (JCA)[2, 3], arevalojc@usal.es

Marzia Malcangio(MM)[1] marzia.malcangio@kcl.ac.uk.

[1]Wolfson CARD, King's College London, SE1 1UL, UK;

[2]Department of Cell Biology and Pathology, Institute of Neurosciences Castilla y León, University of Salamanca, Salamanca, 37007, Spain;

[3]Institute of Biomedical Research of Salamanca, Salamanca, 37007, Spain;

[4]Institute of Cell Biology and Neurobiology, National Research Council and IRCCS Fondazione Santa Lucia, Rome, 00143, Italy.

Corresponding author: Marzia Malcangio, PhD, Wolfson Centre for Age-Related Diseases, Kings College London, Wolfson Wing, Hodgkin Building, Guys Campus, London, SE1 1UL, Email: marzia.malcangio@kcl.ac.uk.

Running title: TrkA signalling is critical for joint pain

Abstract

Objective: Aiming to delineate novel neuro-immune mechanisms for NGF/TrkA signalling in OA pain, we evaluated inflammatory changes in the knee joints following injection of monoiodoacetate (MIA) in mice carrying a TrkA receptor mutation (P782S; TrkA KI mice).

Method: In behavioural studies we monitored mechanical hypersensitivity following intra-articular MIA and oral prostaglandin D_2 (PGD_2) synthase inhibitor treatments. In immunohistochemical studies we quantified joint mast cell numbers, calcitonin gene-related peptide expression in synovia and dorsal root ganglia, spinal cord neuron activation and microgliosis. We quantified joint leukocyte infiltration by flow cytometry analysis, and PGD_2 generation and cyclooxygenase-2 (COX-2) expression in mast cell lines by ELISA and Western blot.

Results: In TrkA KI mice we observed rapid development of mechanical hypersensitivity and amplification of dorsal horn neurons and microglia activation 7 days after MIA. In TrkA KI knee joints we detected significant leukocyte infiltration and mast cells located in the vicinity of synovial nociceptive fibres. We demonstrated that mast cells exposure to NGF results in up-regulation of COX-2 and increase of PGD_2 production. Finally, we observed that a PGD_2 synthase inhibitor prevented MIA-mechanical hypersensitivity in TrkA KI, at doses which were ineffective in WT mice.

Conclusion: Using the trkA KI mouse model, we delineated a novel neuro-immune pathway and suggest that NGF-induced production of PGD_2 in joint mast cells is critical for referred mechanical hypersensitivity in OA, probably through the activation of PGD_2 receptor 1 in nociceptors: TrkA blockade in mast cells constitutes a potential target for OA pain.

Keywords: Prostaglandin D_2; NGF; TrkA; osteoarthritis; mast cells

Introduction

The neurotrophin nerve growth factor (NGF) is constitutively produced and released by synovial fibroblasts in the joint and sensitizes nociceptive neurons that express TrkA receptors and innervate the joints[1]. Under inflammatory conditions, NGF expression is up-regulated by cytokines, and inflammatory cells such as mast cells release NGF[2]. Indeed, extracellular NGF levels are higher in inflamed joints and NGF blockade with both TrkA-IgG fusion protein and NGF monoclonal antibodies produces analgesic effects in preclinical settings[3, 4]. Relevantly, humanised monoclonal anti-NGF antibodies are effective analgesics in people with osteoarthritis joint pain[5]. However, unexpected side effects such as increased incidence of bone necrosis indicate that more studies are needed to understand NGF-mediated regulation of osteoarthritis (OA) pain.

In this preclinical study we use intra-articular monoiodoacetate (MIA) injection as this OA model is associated with dose-dependent and rapid pain-like responses in the ipsilateral limb, which persists for several weeks. The ipsilateral joints display morphological changes of the articular cartilage and bone disruption, which are reflective of some aspects of patient pathology, as well as synovitis and macrophage infiltration[3, 6]. Furthermore, this model of OA reflects specific changes in the NGF/TrkA system as follows: i) the TrkA antagonist AR786 shows both prophylactic and therapeutic anti-nociceptive efficacy in MIA rats[3]; ii) local intra-articular injection of NGF in MIA-knee joints facilitates the responses of spinal cord neurons to extension of the knee joint[7].

The most frequent types of immune cells found in people with OA joints are macrophages, T cells and mast cells[8] TrkA receptors are expressed by mast cells and macrophages and their activation by NGF leads to up-regulation and release of inflammatory mediators, which sensitize joint nociceptors[2].

With the aim to investigate neuro-immune mechanisms mediated by NGF/TrkA signalling in OA pain, we have examined the development of MIA-referred mechanical hypersensitivity and joint pathology in wild type and mice carrying a mutation in the TrkA receptor in which Proline 782 is mutated to Serine. This TrkA mutation confers a defect on ubiquitination by Nedd4-2 (E3 ubiquitin ligase) which leads to i) an increase in NGF-mediated signalling; ii) approximately 30% increase of dorsal root ganglia neurons; iii) increased sensitivity to noxious hot and cold, but not mechanical, stimuli; iv) enhanced behavioural response to intraplantar formalin and v) increased activation of spinal cord neurons after formalin[9, 10].

Method

Animals. Studies were conducted in accordance with UK Home Office regulations, International Association for the Study of Pain and ARRIVE guidelines[11]. Male and female TrkAP782S (TrkA KI) and wild type (WT) littermates of C57BL/6 background, aged 3-6 months old (25-35 g) were housed under a 12-hour light/dark cycle, with food and water available *ad libitum*. In all studies, experimental groups were randomized and an equal number of 3-6 months old-female and -male transgenic mice was used and data combined. Experiments were performed blind.

Behavioural testing. Mechanical withdrawal thresholds were assessed by calibrated von Frey monofilaments (0.02-1g, North Coast Medical Inc.) application to the plantar surface of the hind paw. 50% paw withdrawal threshold (PWT) was determined according to the “up–down” method[12].

In the monoiodoacetate model mice received an intra-articular injection of either saline or 0.7mg MIA (Sigma-Aldrich) in 10µL of sterile saline[6].

Drug administration. A Tanezumab-like antibody (Levicept) or antibody control (IgG1, kappa Sigma-Aldrich, I5154), dissolved in sterile saline were administered subcutaneously at 5mg/kg, every 5 days, starting from the day before MIA injections. HQL-79 (Tocris) was dissolved in 0.5% methylcellulose. HQL-79 (3 and 10mg/kg) or vehicle was administered by oral gavage.

Immunohistochemistry. Seven days after MIA injection, mice were perfuse-fixed under terminal anaesthesia through the ascending aorta with heparinised saline followed by 4% paraformaldehyde fixative solution with 1.5% picric acid in phosphate buffer (0.1M, pH 7.4, PB). Sections from knee joints (30µm), lumbar spinal cord (20µm) and L3-L5 DRG (10µm) were incubated overnight with sheep anti–calcitonin gene-related peptide (CGRP, 1:500, Enzo Life Sciences). Spinal cord sections were incubated as follows: rabbit anti-c-Fos (1:1000, Cell Signaling Technology) followed by Alexa Fluor 488- or 546-conjugated antibodies (1:1000; Molecular Probes); rabbit anti– p-p38 (1:100, Cell Signaling Technology) and biotinylated secondary antibody (1:400 biotin donkey anti-rabbit, Jackson ImmunoResearch Labs); peroxidase containing avidin-biotin complex (1:200, Vector Laboratories) and biotinylated tyramide (NEN Life Science Products) which was detected with ExtrAvidin-FITC (1:500, Sigma-Aldrich); rabbit anti-Iba-1 (1:100 Wako Pure Chemical Industries Ltd.) followed by Alexa Fluor 546-conjugated antibody (1:1000; Molecular Probes). Knee joint sections were incubated with anti-cluster of differentiation 117 (CD117, 1:1000 R&D Systems) or anti–calcitonin gene-related peptide (CGRP). In control experiments, no staining was visible when joint, spinal cord or DRG sections were processed for immunohistochemistry with omission of the primary antibody. All slides were mounted with Vectashield Mounting Medium containing nuclear marker 49,6-diamidino-2-phenylindole·2HCl (DAPI; Vector Laboratories), and visualized using a Zeiss Axioplan 2 fluorescent microscope (Zeiss). Acquisition parameters remained constant and unprocessed images were used for analysis and quantification.

Quantitative assessment of fluorescent intensity. DRG neurons were identified and cell bodies were selected as regions of interest (ROI) using ImageJ software (NIH). At least 200 neurons were sampled, in serial sections at a distance of at least 10 sections (i.e. 100 µm) apart. c-Fos immunoreactivity was determined by counting number of positive profiles within a region defined as laminae I and II, using Axiovision LE 4.8 software (Zeiss). Iba-1 and p-p38 immunoreactivity was determined by counting number of positive profiles within three 2.25 $x10^4$ μm^2 boxes in laminae I-III. Knee joint sections were examined at 10x magnification to identify areas with the highest nerve fibre or cell density in the synovium. The length of nerve fibres was determined by manually tracing them from Z-stack images using Axiovision LE 4.8 software (Zeiss) and reported as density of fibres per volume of synovium – area of synovium x thickness (30µm) - as described previously[13]. $CD117^+$ mast cells were counted and data was expressed as density of cells per volume of synovium[13].

Western blotting. RBL-2H3 cells were homogenized in lysis buffer and 30 mg/ml of protein was loaded on a 10% SDS-PAGE gel. Proteins were wet-transferred using the Bio-Rad system (Bio-Rad Laboratories) and blots were probed overnight with rabbit anti-cyclooxygenase-2 (COX-2) (1:5000; Abcam), incubated with HRP–conjugated anti-rabbit immunoglobulin (Dako) and visualised with BioSpectrum System (Ultra-Violet Products Ltd). Bands were analysed with Quantity One (Bio-Rad Laboratories). β-actin (1:1000; Cell Signaling) was used as loading control.

Flow cytometry. Seven days after OA induction, the skin and muscle were removed and the knee joint isolated with care not to damage the bone and release bone marrow content. Knee joints were digested in serum-free RPMI containing collagenase D (0.5µg/ml) and DNAse (40µg/ml). Isolated cells were incubated with Fc block anti-mouse CD16/CD32 (Clone 2.4G2, BD Biosciences) followed by fluorochrome-conjugated anti-mouse antibodies: CD45.1-Pacific

Blue™ (Clone 30-F11, BioLegend), F4/80-PE (Clone BM8, eBioscience), CD11b-APC (Clone M1/70, eBioscience), CD117-PeCy7 (Clone 2B8, BioLegend) and $Fc_{\varepsilon}RI\alpha$-APC eFluor 780 (Clone MAR 1, eBioscience). Cells were analysed with LSRFortessa™ (BD bioscience) and analyzed with FlowJo software (Tree Start).

Synovial fluid collection. The skin of the knee joint was excised; the patellar ligament was then severed below the patella, which was lifted to expose the synovial membrane. A 30-gauge needle (Micro-Fine insulin syringe; 0.3 ml) was carefully inserted into the knee joint space and gently flushed twice with 25 µl of sterile saline. A total 50 µl of synovial lavage sample was carefully recovered, diluted 1:50 in ELISA buffer, and Prostaglandin D_2 (PGD_2) levels were quantified by MOX ELISA kit (Cayman Chemical, Cambridge, UK).

Cell culture. Rat RBL-2H3 mast cell line (ATCC® CRL-2256™) was plated onto 12-well plates ($1x10^6$cells per well), sensitized for 16h with 100ng/ml anti-DNP IgE (Sigma-Aldrich) and then stimulated with 20ng/ml DNP-BSA (Molecular probes) and 100ng/ml rat β-NGF (R&D Systems) for 0-12h. In some experiments, cells were incubated with DNP-BSA, β-NGF together with LY311727 (Tocris), for 12h. Cell media were used for quantification of PGD_2 by ELISA.

Data Analysis. Data were tested for normal distribution (Shapiro–Wilk test) and analysed for statistical differences using SigmaPlot 13.0 (Systat Software). For behavioural analysis, based on our previous experience and data, in order to achieve alpha 0.05 and power 0.8 we used at least 6 animals per group. Data analysis was performed by two-way repeated measures ANOVA, followed by Tukey test. For immunohistochemical analysis, cell culture and FACS analysis, in order to achieve alpha 0.05 and power 0.8 we used at least 4 samples per group and data were analysed by one way ANOVA followed by Tukey test. The problem of family-wise error rate inflation (inherent in multiple testing) was controlled within each model using

Tukey as post-hoc procedures. Data are expressed as mean±SEM. Results were considered significant when $p<0.05$.

Results

Rapid onset of mechanical hypersensitivity and greater dorsal horn neuron activation and microglial response in the spinal cord of TrkA KI mice after intra-articular MIA

We predicted that a gain in function of TrkA receptors would enhance pain-like behaviour in the MIA model and measured hind paw withdrawal thresholds to mechanical stimulation as baseline values were comparable between TrkA KI and WT mice (Fig. 1A). Furthermore, we used a submaximal dose of MIA (0.7mg/mouse), which in WT mice was associated with slow development of ipsilateral mechanical hypersensitivity starting from day 7 and lasting for up to day 28 as compared to saline controls (Fig 1A). We observed that mechanical hypersensitivity developed more rapidly in TrkA KI and was significantly higher than in WT mice by day 3 post-MIA injection (Fig 1A). Area under the curve (AUC) analysis demonstrated that withdrawal thresholds of MIA-injected TrkA KI mice were lower than WT mice thresholds between days 0 and 7 (Fig. 1B) and days 21 and 28 after MIA injection (Fig. 1C).

To confirm that nerve growth factor (NGF) contributed to mechanical hypersensitivity in TrkA KI mice, we administered a tanezumab-like antibody that prevented the development of mechanical hypersensitivity throughout the duration of the study (14 days) compared to vehicle treatment (Fig. 1D and E). Similarly, the antibody prevented the development of mechanical hypersensitivity in WT mice (Suppl. Fig. 1).

Consistent with an increased afferent input to the dorsal horn of the spinal cord in the MIA model[6], we counted more c-Fos-expressing neurons in ipsilateral laminae I-II at day 7 MIA

compared to saline (Fig. 2A, B and E). In addition, the number of c-Fos$^+$ cells was higher in TrkA KI than WT dorsal horns (Fig. 2B, D and E). Similarly, Iba-1$^+$ microglial cell number was higher in ipsilateral dorsal horn of MIA compared to saline WT mice (Fig. 2F, G and J) and even higher in MIA-TrkA KI dorsal horns (Fig. 2G, I and J). Furthermore, phosphorylated p38 in Iba-1$^+$microglia was significantly higher in ipsilateral dorsal horn of MIA- compared to saline-treated TrkA KI mice (Fig. 2H, I and K). No contralateral microglia changes were observed in either WT or TrkA KI spinal cords (data not shown).

These data indicate that the responses of central neurons and microglia to peripheral tissue injury are amplified in TrkA KI conditions and these central changes are associated with the faster on-set of OA pain-related behaviour in TrkA KI compared to WT mice.

Higher number of inflammatory cells in the MIA knee joint of TrkA KI mice

As we were interested in exploring novel neuro-immune mechanisms that would involve the NGF-TrkA signalling in the joint, we examined the extent of synovial inflammation, which is associated with MIA pain phenotype more than cartilage degradation[3].

Indeed, 7 days after MIA injection, no signs of cartilage degradation were observed in either WT or TrkA KI joints (Fig. 3A). However, both synovial volume and density of CGRP-expressing fibres were higher in MIA compared to saline groups (Fig. 3B, C, D and E). We noticed that, under normal conditions (saline-treated mice), CGRP-fibres density in TrkA KI was higher than in WT synovia (Fig. 3C, D and E). Consistent with higher expression of CGRP in peptidergic fibres[9], the cell bodies of TrkA KI sensory fibres expressed more CGRP than WT fibres (Fig. 3F, G, H and I) and CGRP increased significantly 7 days after MIA injection in both WT and TrkA KI (Fig. 3F, G, H and I), suggesting that this peptide is up-regulated as a result of MIA-induced inflammation in the joints.

Although synovial fibre density and volume changes were comparable between TrkA KI and WT, flow cytometry analysis of cells isolated from the knee joints revealed that inflammatory cells numbers were not altered on day 7 after MIA injection in WT tissue, but samples of MIA-TrkA KI ipsilateral joints contained a significant higher numbers of leukocytes ($CD45^+$ cells) (Fig. 4B, D and E), macrophages ($F4/80^+CD11b^+$ cells) (Fig. 4B, D and F) and mast cells ($CD117^+$ and $FC\varepsilon RI^+$) (Fig. 4B, D and G).

Consistent with the flow cytometry data, there were more CD117 immunoreactive cells (marker for both $CD117^+FC\gamma RI^+$ and $CD117^+FC\gamma RI^-$ mast cells) in the synovia of MIA-TrkA KI joints than in synovia of TrkA KI saline controls (Fig 5C, D and E).

No changes in mast cells numbers were observed in WT synovia between saline and MIA-treated groups (Fig. 5A, B and E). Intriguingly, in the synovia of TrkA KI joints, more mast cells were located in the vicinity of CGRP-positive fibres compared to both TrkA KI saline controls and MIA WT joints (Fig. 5B, C, D and F). Thus, on day 7 after a submaximal MIA dose the cellular infiltrate reaches measurable levels in TrkA KI knee joints, which cannot be detected under WT conditions.

NGF up-regulates COX-2 which mediates a delayed PGD_2 formation in mast cells

MIA-associated synovial inflammation is amplified under TrkA KI conditions and provides a model setting to investigate neuro-immune mechanisms that are driven by NGF. As mast cells that accumulated close to sensory fibres can express TrkA receptors, we tested the hypothesis that NGF activation of mast cells leads to the release of mediators, which can sensitise nociceptive fibres. We confirmed existing data[14] and observed that NGF stimulates the generation of PGD_2 in basophilic leukaemia cell line RBL-2H3, which is known to resemble

mast cells[15]. Specifically, 12h after antigen (DNP-BSA)-dependent stimulation, a significant increase of PGD_2 levels over basal values was quantified in the media (Fig. 6A). The presence of NGF with DNP-BSA in the culture media resulted in higher PGD_2 levels 8h after antigen stimulation and levels remained elevated at the 12h time-point (Fig. 6A). Thus, NGF increases $FC\varepsilon RI$-induced production of PGD_2 in culture and we know that PLA_2 is required for NGF-induced delayed PGD_2 generation[12]. We, therefore, we tested the effect of phospholipase A_2 (PLA_2) inhibitor LY311727 on NGF-induced PGD_2 generation, 12h after incubation - the time-point at which differences in PGD_2 generation between experimental groups were more pronounced. LY311727 (1-100µM) inhibited NGF-induced PGD_2 generation, in a concentration-dependent manner (Fig. 6B). Indeed, when cells were stimulated with DNP-BSA and NGF, the levels of PGD_2 released in the media were higher than when cells were stimulated with DNP-BSA alone (Fig. 6B). The presence of 1µM LY311727 had no effect on either DNP-BSA or DNP-BSA with NGF-induced PGD_2 generation (Fig. 6B). LY311727 (10µM) had no effect on DNP-BSA induced generation of PGD_2 but reduced the level of PGD_2 generated by the antigen together with NGF (Fig. 6B). At 100µM, LY311727 reduced the generation of PGD_2 induced by both antigen and antigen together with NGF (Fig. 6B).

Whilst the initial phase of PGD_2 generation is dependent on constitutively expressed COX-1, the second phase is dependent on the induction of COX-2 mRNA and protein[14, 16]. We, therefore, quantified COX-2 after cells were incubated with DNP-BSA alone or together with NGF and found that LY311727 (10µM) significantly reduced NGF-induced expression of COX-2, but not in cells incubated with antigen alone (Fig. 6C and D). At 100µM, LY311727 reduced COX-2 protein levels in cells stimulated with either antigen alone or antigen together with NGF (Fig. 6C and D). Altogether, these results confirm that NGF induces up-regulation of COX-2 that results in delayed PGD_2 formation in mast cells.

PGD_2 synthase inhibitor HQL-79 prevents MIA-induced mechanical hypersensitivity in TrkA KI mice

PGD_2 is known to exert pro-nociceptive effects through the activation of PGD_2 receptor 1 (DP_1) and 2 (DP_2) receptors expressed by sensory neurons, which potentiate the amplitude of tetrodotoxin-resistant (TTX-R) Na^+ currents[17]. Therefore, NGF-induced production of PGD_2 in mast cells could mediate the pro-nociceptive effect of NGF in TrkA KI joints in which a significant number of mast cells are located in the vicinity of sensory neurons. To test this possibility we evaluated the effect of the PGD_2 synthase inhibitor HQL-79 on MIA-induced hypersensitivity. We used an inhibitor acting downstream of the PGD_2 synthesis cascade in order to avoid non-specific effects on other bioactive prostaglandins. When WT and TrkA KI mice were administered with either 3 or 10mg/kg of HQL-79 daily, for 8 days, starting from the day of the MIA injection, we observed a dose-dependent reduction of mechanical thresholds (Fig. 6E). On the last experimental day the lowest dose of HQL-79 (3mg/kg) reversed MIA-induced hypersensitivity in TrkA KI, but not WT mice (Fig. 6E). However, at the higher dose of 10mg/kg, HQL-79 induced similar reversal of MIA-induced mechanical hypersensitivity in TrkA KI and WT mice (Fig. 6E). Next, we evaluated whether HQL-79 treatment had affected PGD_2 synthesis in the damaged tissue and measured PGD_2 levels in knee joints lavages. We observed that at 7 days after MIA injection, the levels of PGD_2 were significantly higher in TrkA KI than WT joint lavages (Fig 6F). After treatment with 3mg/kg of HQL-79, PGD_2 joint levels were significantly lower than in vehicle treated, in TrkA KI but not in WT samples (Fig. 6F). However, a higher dose of HQL-79 (10mg/kg) reduced PGD_2 levels in both WT and TrkA KI joints (Fig. 6F). These data indicate that an increased production of PGD_2 in the knee joint is critical for the development of mechanical hypersensitivity in TrkA KI mice.

Discussion

In this study, we have identified a novel pathway that highlights the critical contribution of the NGF/TrkA system to the initiation of mechanical allodynia in a model of OA pain. Using the TrkA KI mouse model, which amplifies changes in MIA-associated inflammation, we reveal mechanisms that could not be detected in WT conditions at the dose of MIA selected for these studies.

Our *in vitro* findings suggest that, in OA joints, extracellular NGF acts via TrkA receptor activation in mast cells and results in significant up-regulation of COX-2 and generation of PGD_2. This prostaglandin can then sensitise sensory neurons through the activation of DP_1 receptors[17], which facilitate noxious signalling from the OA joint to the dorsal horn of the spinal cord. Thus, this mast cell-to-nociceptors communication involves an anatomical relationship and includes PGD_2 as an essential mediator in the cascade of events that acts downstream of TrkA activation on mast cells, sensitizing nociceptors via DP_1 receptor activation. The pathway described here represents a novel signalling module that underlies interactions between mast cells and nociceptive neurons in eliciting OA-pain hypersensitivity (Fig. 7). Our data indicate no occurrence of gender differences whereas significant gender variance applies to immune cell response in the spinal cord after peripheral nerve injury[18].

The knee joints are innervated by primary afferent fibres whose cell bodies are located in the lumbar DRG[6, 19]. A significant proportion of these joint afferents, in both humans and animals are peptidergic and some of them express TrkA receptors[19, 20]. Both CGRP and substance P (SP) are up-regulated in DRG under peripheral inflammatory conditions as well as after MIA injection in the knee, which also results in elevation of TrkA mRNA levels in DRG[19, 21] .We observed that a TrkA mutation, which increases receptor signalling, is associated with a significant increase in both number of neurons and percentage of CGRP-expressing neurons in TrkA KI DRG[9]. Such changes can be explained by the following evidence: i) most DRG neurons depend on NGF-TrkA signalling for survival during development ; ii) null mutations of NGF and TrkA are associated with substantial loss of sensory neurons iii) CGRP levels in sensory neurons are under NGF regulation[22].

In this study, under TrkA KI conditions, the responses to primary afferent input from the joint of both dorsal horn neurons and microglia were magnified and indicated the occurrence of central sensitization. Indeed, MIA injection in the knee is associated with an increased release of peptides from primary afferent fibres in the dorsal horns and intrathecal CGRP antagonists can reverse established MIA referred allodynia[6]. Following MIA treatment, dorsal horn neurons with input from the joints demonstrate expansion of their peripheral receptive fields and intra-articular NGF injection, at a dose previously shown to produce pain behaviour, increases both responses and peripheral receptive fields of spinal neurons in untreated and, to a larger extent, in MIA-treated rats[21]. Together, these data suggest that engagement of the NGF/TrkA system is associated with a spinal sensitization[7]. Relevantly, the spreading of pain to sites distant from the joint has been reported in OA patients and central sensitisation is believed to underlie such change[23, 24].

There is increasing evidence that inflammation is present in synovial tissue of OA patients and synovitis is associated with pain in human OA[23, 25]. Extracellular NGF at the periphery acts on TrkA receptors expressed by peptidergic fibres, increasing inflammation and neuropeptide release from sensory nerves[19, 26]. Furthermore, intra-articular NGF can increase synovitis and the number of inflammatory cells, including macrophages and mast cells, in the synovium[21]. Consistently, blockade of TrkA receptor signalling reduces synovitis in MIA-induced OA[3].

Mast cells are elevated in joints of OA compared to rheumatoid arthritis patients suggesting a specific role of these cells in the pathophysiology of OA[27]. There are several mechanisms by which mast cells can contribute to the pathology of OA, namely by attracting other immune cells through cytokine and chemokine release[2]. Further, mast cells can contribute to pain in OA by releasing soluble mediators and enzymes[2]. In this study we focused on the latter mechanism, as we observed a close anatomical relationship between mast cells and

peptidergic fibres in the synovia. A similar anatomical arrangement has been reported previously whereby mast cells and peptidergic fibres form a functional unit involved in the axon reflex[2]. Particularly, NGF-induced inflammation in non-articular tissues involves mast cell degranulation[2, 22]. NGF has been suggested to exert a direct role on mast cell development and function and bone marrow derived mast cells from TrkA knock out mice show decrease degranulation in comparison to bone marrow derived mast cells from control mice[28, 29]. NGF can drive the synthesis of PGD_2[14, 16], which is synthesised by COX-1 and 2, and is the main prostaglandin released by mast cells. In this study, we observed that NGF induced PGD_2 production by mast cells through the induction of mast cell COX-1/2 expression. PGD_2 receptors, namely DP_1 receptors, are expressed by nociceptive fibres, where they can increase CGRP release and bradykinin-induced SP release as well as the amplitude of TTX-R sodium currents[17, 30]. Here we observed that a PGD_2 synthase inhibitor prevented both development of MIA-induced mechanical hypersensitivity and PGD_2 accumulation in the knee joint, providing further support to a role of mast cell-derived PGD_2 in modulation of nociceptive signalling.

In conclusion, anti-NGF therapies have shown promising analgesic potential for OA pain treatment. However, the presence of significant adverse effects on the joint structure calls for a better understanding of the mechanisms by which NGF-TrkA signalling participate in OA pain. Here we suggest that blockade of TrkA in mast cells constitutes a potential target for OA pain. For instance selectivity could be achieved through the development of bispecific antibodies[31] where the second arm targets both TrkA and a mast cell specific antigen.

Authors' contributions

JSV, JCA and MM designed the research. JSV, VV, LC and RS performed the experiments and collected the data. JSV, VV and RS analysed data. JSV and MM wrote the paper. All authors read and approved the submitted manuscript.

Role of the funding source

This work was supported EC FP7 PAINCAGE grant 603191. This funding source had no influence on study design, data acquisition, analysis or manuscript preparation.

Competing interests

The authors declare no competing financial interests.

Acknowledgements

The authors would like to thank Dr Simon Westbrook from Levicept Ltd. (Kent, UK) for kindly gifting the anti-NGF antibody used in this study. The authors would also like to thank Dr Silvia Ferrer, Mr Carl Hobbs, Dr Julie Keeble, Mr Tom Pitcher and Miss Julia Sanchez for assistance with these studies.

References

1. Manni L, Lundeberg T, Fiorito S, Bonini S, Vigneti E, Aloe L. Nerve growth factor release by human synovial fibroblasts prior to and following exposure to tumor necrosis factor-alpha, interleukin-1 beta and cholecystokinin-8: the possible role of NGF in the inflammatory response. Clin Exp Rheumatol 2003; 21: 617-624.

2. Skaper SD. Nerve growth factor: a neuroimmune crosstalk mediator for all seasons. Immunology 2017; 151: 1-15.

3. Nwosu LN, Mapp PI, Chapman V, Walsh DA. Blocking the tropomyosin receptor kinase A (TrkA) receptor inhibits pain behaviour in two rat models of osteoarthritis. Ann Rheum Dis 2016; 75: 1246-1254.

4. Xu L, Nwosu LN, Burston JJ, Millns PJ, Sagar DR, Mapp PI, et al. The anti-NGF antibody muMab 911 both prevents and reverses pain behaviour and subchondral osteoclast numbers in a rat model of osteoarthritis pain. Osteoarthritis Cartilage 2016; 24: 1587-1595.

5. Lane NE, Schnitzer TJ, Birbara CA, Mokhtarani M, Shelton DL, Smith MD, et al. Tanezumab for the treatment of pain from osteoarthritis of the knee. N Engl J Med 2010; 363: 1521-1531.

6. Ogbonna AC, Clark AK, Gentry C, Hobbs C, Malcangio M. Pain-like behaviour and spinal changes in the monosodium iodoacetate model of osteoarthritis in C57Bl/6 mice. Eur J Pain 2013; 17: 514-526.

7. Sagar DR, Nwosu L, Walsh DA, Chapman V. Dissecting the contribution of knee joint NGF to spinal nociceptive sensitization in a model of OA pain in the rat. Osteoarthritis Cartilage 2015; 23: 906-913.

8. de Lange-Brokaar BJ, Ioan-Facsinay A, van Osch GJ, Zuurmond AM, Schoones J, Toes RE, et al. Synovial inflammation, immune cells and their cytokines in osteoarthritis: a review. Osteoarthritis Cartilage 2012; 20: 1484-1499.

9. Yu T, Calvo L, Anta B, Lopez-Benito S, Lopez-Bellido R, Vicente-Garcia C, et al. In vivo regulation of NGF-mediated functions by Nedd4-2 ubiquitination of TrkA. J Neurosci 2014; 34: 6098-6106.

10. Yu T, Calvo L, Anta B, Lopez-Benito S, Southon E, Chao MV, et al. Regulation of trafficking of activated TrkA is critical for NGF-mediated functions. Traffic 2011; 12: 521-534.

11. Kilkenny C, Browne WJ, Cuthill IC, Emerson M, Altman DG. Improving bioscience research reporting: the ARRIVE guidelines for reporting animal research. Osteoarthritis Cartilage 2012; 20: 256-260.

12. Pitcher T, Sousa-Valente J, Malcangio M. The Monoiodoacetate Model of Osteoarthritis Pain in the Mouse. J Vis Exp 2016. doi: 10.3791/53746.

13. Jimenez-Andrade JM, Mantyh PW. Sensory and sympathetic nerve fibers undergo sprouting and neuroma formation in the painful arthritic joint of geriatric mice. Arthritis Res Ther 2012; 14: R101.

14. Tada K, Murakami M, Kambe T, Kudo I. Induction of cyclooxygenase-2 by secretory phospholipases A2 in nerve growth factor-stimulated rat serosal mast cells is facilitated by interaction with fibroblasts and mediated by a mechanism independent of their enzymatic functions. J Immunol 1998; 161: 5008-5015.

15. Seldin DC, Adelman S, Austen KF, Stevens RL, Hein A, Caulfield JP, et al. Homology of the rat basophilic leukemia cell and the rat mucosal mast cell. Proc Natl Acad Sci U S A 1985; 82: 3871-3875.

16. Murakami M, Tada K, Nakajima K, Kudo I. Cyclooxygenase-2-dependent delayed prostaglandin D2 generation is initiated by nerve growth factor in rat peritoneal mast cells: its augmentation by extracellular type II secretory phospholipase A2. J Immunol 1997; 159: 439-446.

17. Ebersberger A, Natura G, Eitner A, Halbhuber KJ, Rost R, Schaible HG. Effects of prostaglandin D2 on tetrodotoxin-resistant Na+ currents in DRG neurons of adult rat. Pain 2011; 152: 1114-1126.

18. Sorge RE, Mapplebeck JC, Rosen S, Beggs S, Taves S, Alexander JK, et al. Different immune cells mediate mechanical pain hypersensitivity in male and female mice. Nat Neurosci 2015; 18: 1081-1083.

19. Ferreira-Gomes J, Adaes S, Sarkander J, Castro-Lopes JM. Phenotypic alterations of neurons that innervate osteoarthritic joints in rats. Arthritis Rheum 2010; 62: 3677-3685.

20. Saito T, Koshino T. Distribution of neuropeptides in synovium of the knee with osteoarthritis. Clin Orthop Relat Res 2000; 376: 172-182.

21. Ashraf S, Mapp PI, Burston J, Bennett AJ, Chapman V, Walsh DA. Augmented pain behavioural responses to intra-articular injection of nerve growth factor in two animal models of osteoarthritis. Ann Rheum Dis 2014; 73: 1710-1718.

22. Pezet S, McMahon SB. Neurotrophins: mediators and modulators of pain. Annu Rev Neurosci 2006; 29: 507-538.

23. Stoppiello LA, Mapp PI, Wilson D, Hill R, Scammell BE, Walsh DA. Structural associations of symptomatic knee osteoarthritis. Arthritis Rheumatol 2014; 66: 3018-3027.

24. Lluch E, Torres R, Nijs J, Van Oosterwijck J. Evidence for central sensitization in patients with osteoarthritis pain: a systematic literature review. Eur J Pain 2014; 18: 1367-1375.

25. Walsh DA, Yousef A, McWilliams DF, Hill R, Hargin E, Wilson D. Evaluation of a Photographic Chondropathy Score (PCS) for pathological samples in a study of inflammation in tibiofemoral osteoarthritis. Osteoarthritis Cartilage 2009; 17: 304-312.

26. Saxler G, Loer F, Skumavc M, Pfortner J, Hanesch U. Localization of SP- and CGRP-immunopositive nerve fibers in the hip joint of patients with painful osteoarthritis and of patients with painless failed total hip arthroplasties. Eur J Pain 2007; 11: 67-74.

27. de Lange-Brokaar BJ, Kloppenburg M, Andersen SN, Dorjee AL, Yusuf E, Herb-van Toorn L, et al. Characterization of synovial mast cells in knee osteoarthritis: association with clinical parameters. Osteoarthritis Cartilage 2016; 24: 664-671.

28. Coppola V, Barrick CA, Southon EA, Celeste A, Wang K, Chen B, et al. Ablation of TrkA function in the immune system causes B cell abnormalities. Development 2004; 131: 5185-5195.

29. Matsuda H, Kannan Y, Ushio H, Kiso Y, Kanemoto T, Suzuki H, et al. Nerve growth factor induces development of connective tissue-type mast cells in vitro from murine bone marrow cells. J Exp Med 1991; 174: 7-14.

30. Isensee J, Wenzel C, Buschow R, Weissmann R, Kuss AW, Hucho T. Subgroup-elimination transcriptomics identifies signaling proteins that define subclasses of TRPV1-positive neurons and a novel paracrine circuit. PLoS One 2014; 9: e115731.

31. Ferrari M, Onuoha SC, Pitzalis C. Trojan horses and guided missiles: targeted therapies in the war on arthritis. Nat Rev Rheumatol 2015; 11: 328-337.

Legends

Figure 1. MIA-induced mechanical hypersensitivity develops faster in TrkA KI mice**. A**, Mechanical thresholds assessed as paw withdrawal thresholds (PWT) following intra-articular injection of monoiodoacetate (MIA) (0.7 mg/mouse) or saline (10 µl/mouse) to wild type (WT) or TrkAP782S mice (TrkA KI). Values are mean ± SEM, *n*=9-12 mice/group. *p<0.05, ***p<0.001 versus saline control or versus WT MIA. Two-way repeated measures (RM) ANOVA followed by post-hoc Tukey test. There is a statistically significant interaction between factors (P<0.001) **B,** Areas under the curve (AUC) for ipsilateral PWT from day 0 to 7 after MIA injection. **C,** AUC for ipsilateral PWT from days 21 to 28 after MIA injection. Values are mean ± SEM. *p<0.05, *** p<0.001, versus saline control group or versus WT MIA; one-way ANOVA post-hoc Tukey test. **D,** Mechanical thresholds (PWT) following intra-articular injection of MIA (0.7mg/mouse) or saline (10 µl/mouse). On days -1, 4 and 9 mice were treated with Tanezumab-like antibody (Ab) or control Ab (5mg/kg s.c.) (Sigma I5154). Values are mean ±SEM of 6-9 mice/group. ***p< 0.001; **p<0.01 versus saline Tanezumab-like Ab group or versus TrkA KI MIA control Ab group. Two-way RM ANOVA post-hoc Tukey test. There is a statistically significant interaction between factors (P<0.001) **E,** AUC for ipsilateral PWT. Values are mean±SEM. *** p<0.001, versus saline Tanezumab-like Ab group or versus MIA control Ab group; one-way ANOVA post-hoc Tukey test.

Figure 2. Greater dorsal horn neuron activation and microglia response in the lumbar spinal cord of TrkA KI mice at 7 days after MIA. **A-D**, c-Fos immunoreactivity in the dorsal horn Scale bar 200 µm. **E**, Quantification of c-Fos immunoreactivity in laminae I and II (size of area: $6x10^4$ μm^2). **F-I**, Iba1 (red) and p-p38 (green) immunoreactivity in the ipsilateral dorsal horn. Scale bars 100 µm. **J** and **K**, Quantification of Iba1 (**J**) and p-p38/Iba1 (**K**) immunoreactivity in the ipsilateral dorsal horn (size of area: $2.25x10^4$ μm^2). Values are mean ± SEM. * p<0.05, **

p<0.01, ***p<0.001 versus saline control or versus WT MIA, one-way ANOVA, post-hoc Tukey test. *n*=4-6.

Figure 3. Osteoarthritis pathology and CGRP expression in DRG 7 days after MIA injection. **A** Quantitative scoring of osteoarthritis joint pathology **B-C**, Quantification of both synovial volume **B**) and CGRP immunopositive fibre density (**C**) in MIA or saline injected joints of WT or TrkA KI mice. **D-E**, $CGRP^+$ fibres in ipsilateral knee joint synovium of WT (**D**) and TrkA KI (**E**). **F-G,** Expression of CGRP immunoreactivity in L3 DRG of WT (**F**) and TrkA (**G**) Scale bar 50 µm. **H-I**, Percentage of $CGRP^+$ small (**I**, <21 µm) and medium (**J**, 21-36 µm) diameter neurons in L3 DRG. Values are mean ± SEM. *p< 0.05; **p<0.01; ***p<0.001 versus WT saline or versus TrkA KI MIA, one-way ANOVA, post-hoc Tukey test. *n*=4.

Figure 4. Significant number of inflammatory cells in knee joint of TrkA KI mice 7 days after MIA. **A-D**, Representative dot-plot/FACS plots analysis of $CD45^+$ cells (left panels), $F4/80^+$ and $CD11b^+$ cells (centre panels) and $CD117^+$ and $FC\varepsilon RI^+$ cells (right panels) in ipsilateral knee joints. **E-G**, Quantification of leukocytes (**E**), macrophages (**F**) and mast cells (**G**) in synovial fluid. Values are mean ± SEM; *n*=4-7 per experimental group. ** p<0.01 *** p<0.001 versus saline control; One-way ANOVA post hoc Tukey test.

Figure 5. Significant number of mast cells in vicinity of nociceptive fibres, in TrkA KI joints 7 days after MIA. **A-D**, $CD117^+$ cells and $CGRP^+$ fibres in ipsilateral knee joint synovia. Scale bars 50 µm. **E-F**, Quantification of total number of mast cells (**E**) and number of mast cells in close proximity (<5 µm) to CGRP fibres (**F**) in synovia of MIA or saline injected joints of WT or TrkA KI mice. Values are mean ± SEM; *n*=4 per experimental group. *p<0.05, **p<0.01, versus control group or versus WT MIA one-way ANOVA post hoc Tukey test.

Figure 6. NGF induces PGD_2 synthesis in mast cells and inhibition of PGD_2 in the knee joint is associated with prevention of MIA-induced mechanical hypersensitivity. **A**, Time course of PGD_2 generation. RBL-2H3 cells were stimulated with DNP-BSA (20 ng/ml, black bars) or DNP-BSA with 100 ng/ml NGF (white bars). Values are mean ± SEM, *n*=4-8. *p<0.05, **p<0.01 ***p<0.001 versus baseline values or versus antigen alone. One-way ANOVA post-hoc Tukey's test. **B-D**, Effects of PLA_2 inhibitor LY311727 on PGD_2 generation (**B**) and COX-2 protein levels (**C-D**). RBL-2H3 cells were stimulated for 12h with DNP-BSA (20 ng/ml, black bars) or DNP-BSA with 100 ng/ml NGF (white bars) in the presence of LY311727. Values are mean ± SEM, *n*=6. *p<0.05, *** p<0.001 compared to no PLA_2 inhibitor control or versus antigen alone. **E-F,** Dose-dependent reversal of mechanical hypersensitivity by prolonged oral administration of HQL-79 (3 and 10 mg/kg); vehicle control 0.5% methyl-cellulose. **E,** Percentage reversal assessed on day 7 post-MIA injection. **F,** HQL-79 reduced the levels of PGD_2 recovered from the synovial fluid of MIA-injected knee joints, in a dose dependent manner. Values are mean ± SEM, *n*=6-16. *p<0.05, ** p<0.01 compared to no inhibitor control or versus WT mice. One-way ANOVA post-hoc Tukey test.

Figure 7. Proposed model describing the pathway through which PGD_2 generated by mast cells in response to elevation in NGF levels leads to an increase of nociceptive signalling in OA joints. Extracellular NGF produced in response to inflammation activates TrkA receptors in mast cells and facilitates PGD_2 formation in two ways i) by promoting the translocation of PLA_2 from cytoplasm to endoplasmic reticulum, where PLA_2 releases arachidonic acid (AA) from membrane phospholipids and ii) by inducing expression of COX-2 which mediates the synthesis of PGD_2 precursor PGH_2 from AA. PGD_2 can exert a pro-nociceptive effect through the activation of DP_1 receptors expressed by sensory neurons, which activate sodium channels thereby increasing afferent input to the dorsal horn of the spinal cord.

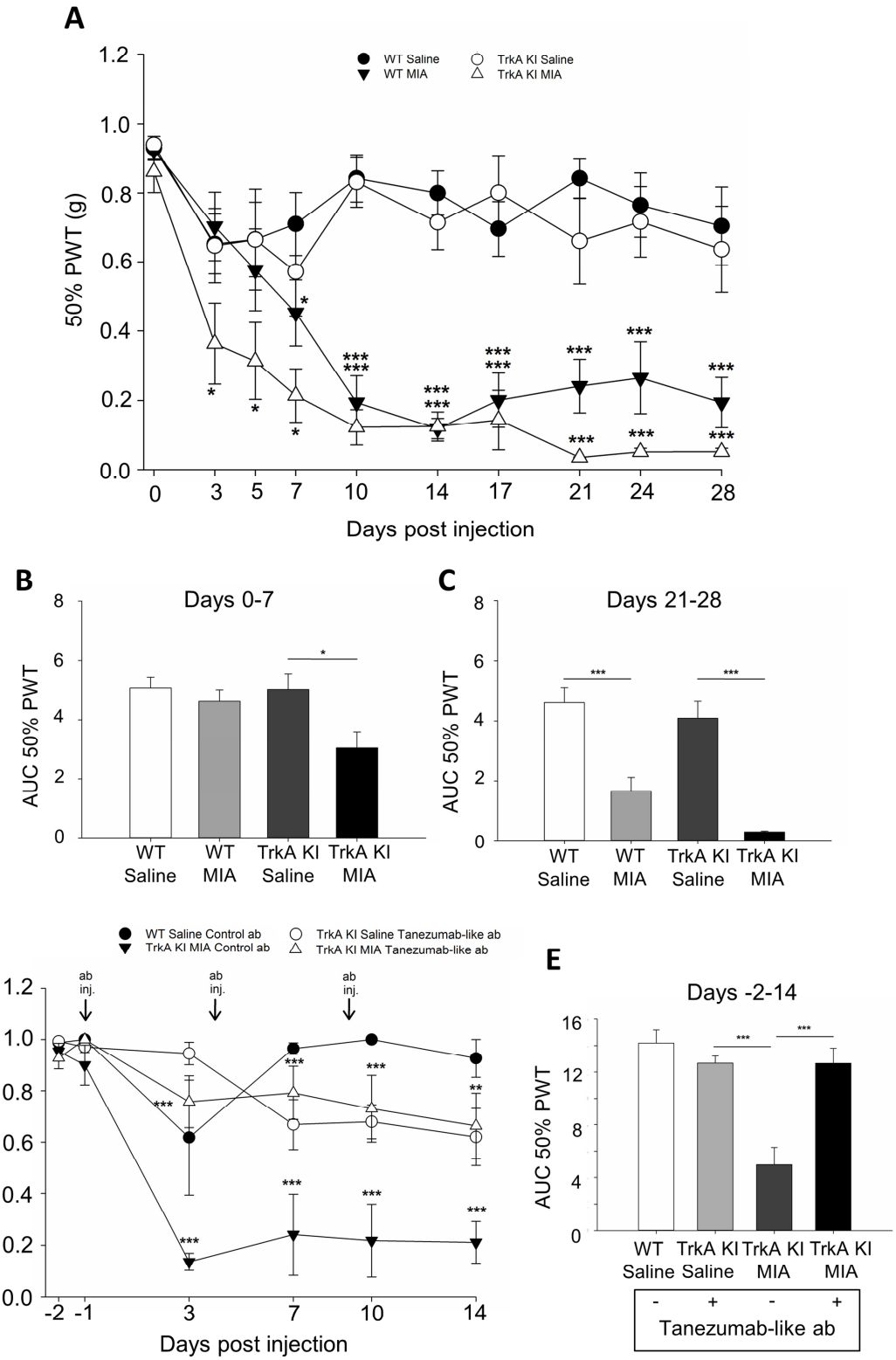
A
WT Saline
WT MIA
TrkA KI Saline
TrkA KI MIA
50% PWT (g)
Days post injection
B
Days 0-7
AUC 50% PWT
WT Saline
WT MIA
TrkA KI Saline
TrkA KI MIA
C
Days 21-28
AUC 50% PWT
WT Saline
WT MIA
TrkA KI Saline
TrkA KI MIA
D
WT Saline Control ab
TrkA KI MIA Control ab
TrkA KI Saline Tanezumab-like ab
TrkA KI MIA Tanezumab-like ab
ab inj.
50% PWT (g)
Days post injection
E
Days -2-14
AUC 50% PWT
WT Saline
TrkA KI Saline
TrkA KI MIA
TrkA KI MIA
Tanezumab-like ab

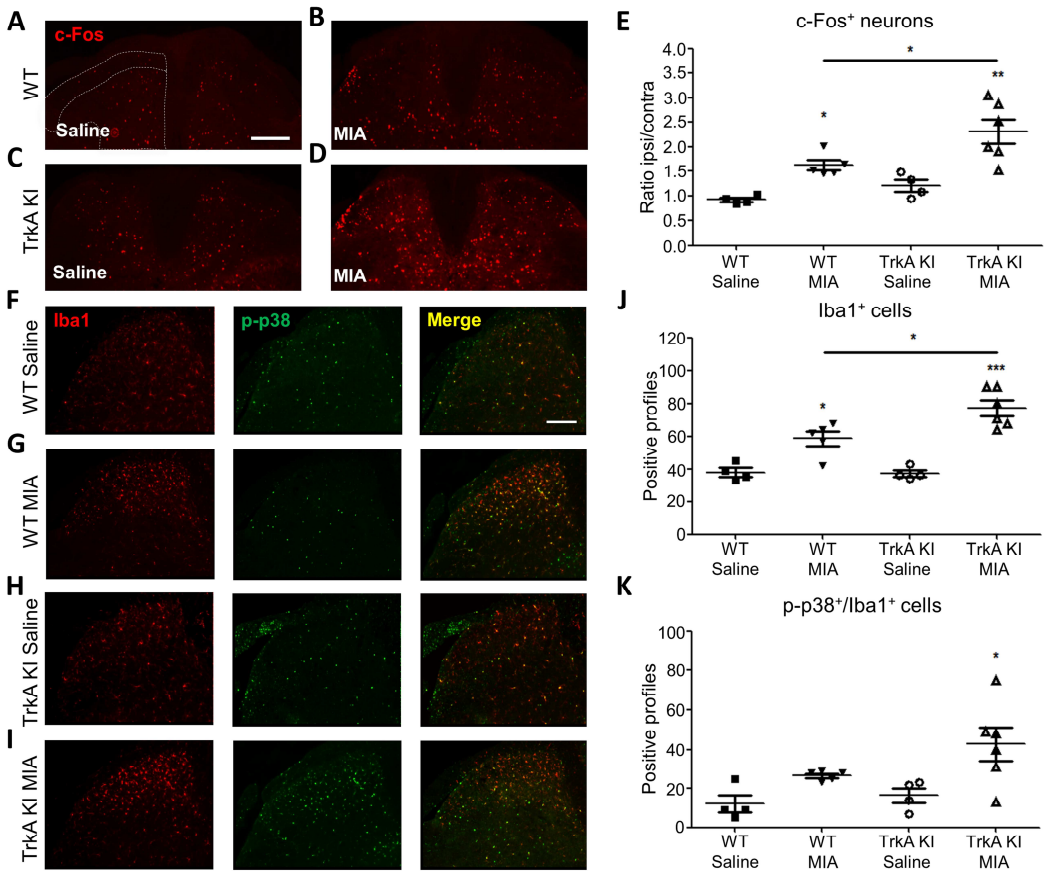
A
c-Fos
WT
Saline
B
MIA
C
TrkA KI
Saline
D
MIA
E
c-Fos⁺ neurons
Ratio ipsi/contra
WT Saline
WT MIA
TrkA KI Saline
TrkA KI MIA
F
Iba1
p-p38
Merge
WT Saline
G
WT MIA
H
TrkA KI Saline
I
TrkA KI MIA
J
Iba1⁺ cells
Positive profiles
K
p-p38⁺/Iba1⁺ cells

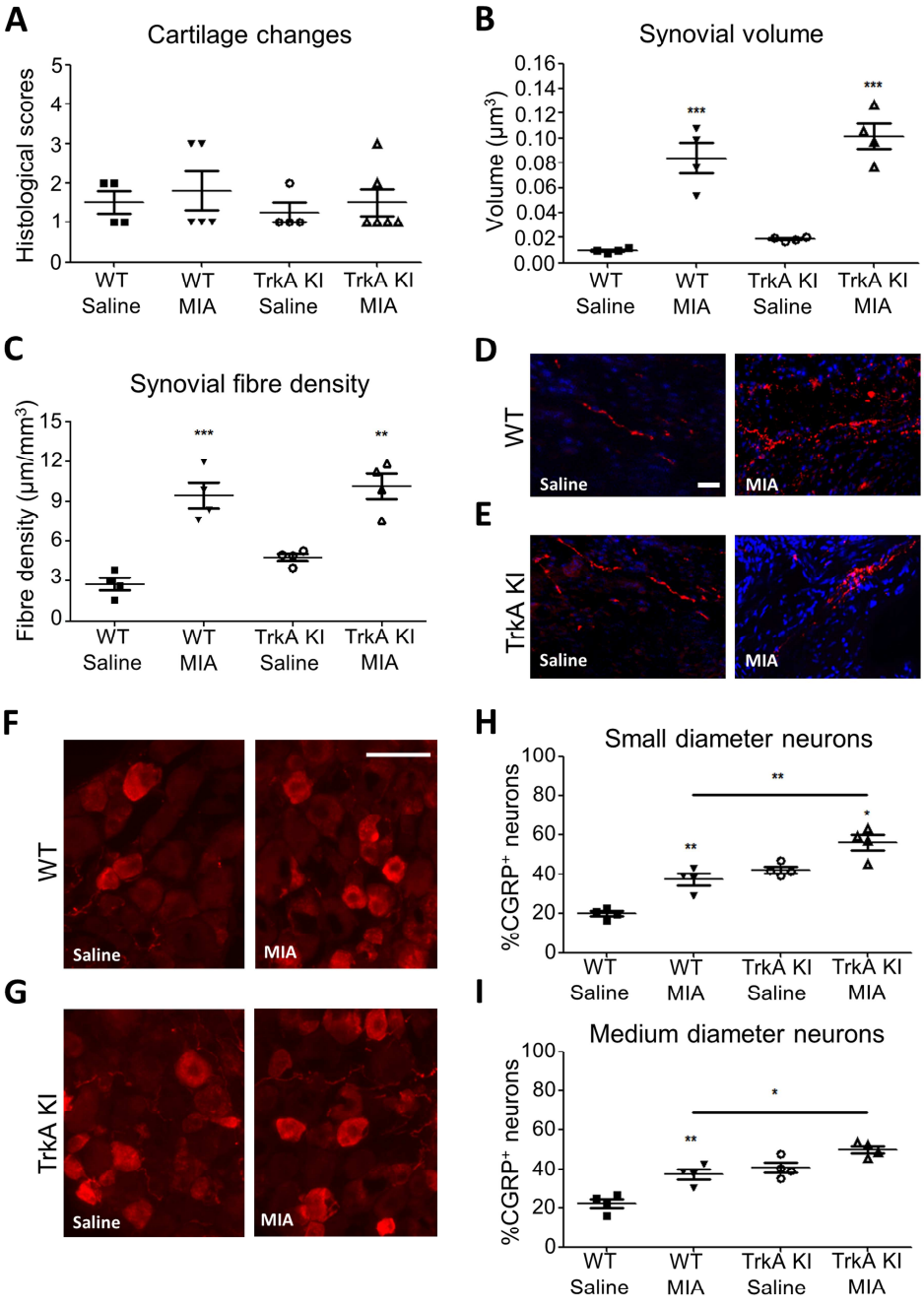
A
Cartilage changes
Histological scores
0
1
2
3
4
5
WT Saline
WT MIA
TrkA KI Saline
TrkA KI MIA
B
Synovial volume
Volume (µm3)
0.00
0.02
0.04
0.06
0.08
0.10
0.12
0.14
0.16
***
***
C
Synovial fibre density
Fibre density (µm/mm3)
0
3
6
9
12
15
***
**
D
WT
Saline
MIA
E
TrkA KI
Saline
MIA
F
WT
Saline
MIA
G
TrkA KI
Saline
MIA
H
Small diameter neurons
%CGRP+ neurons
0
20
40
60
80
100
**
**
*
I
Medium diameter neurons
%CGRP+ neurons
0
20
40
60
80
100
**
*

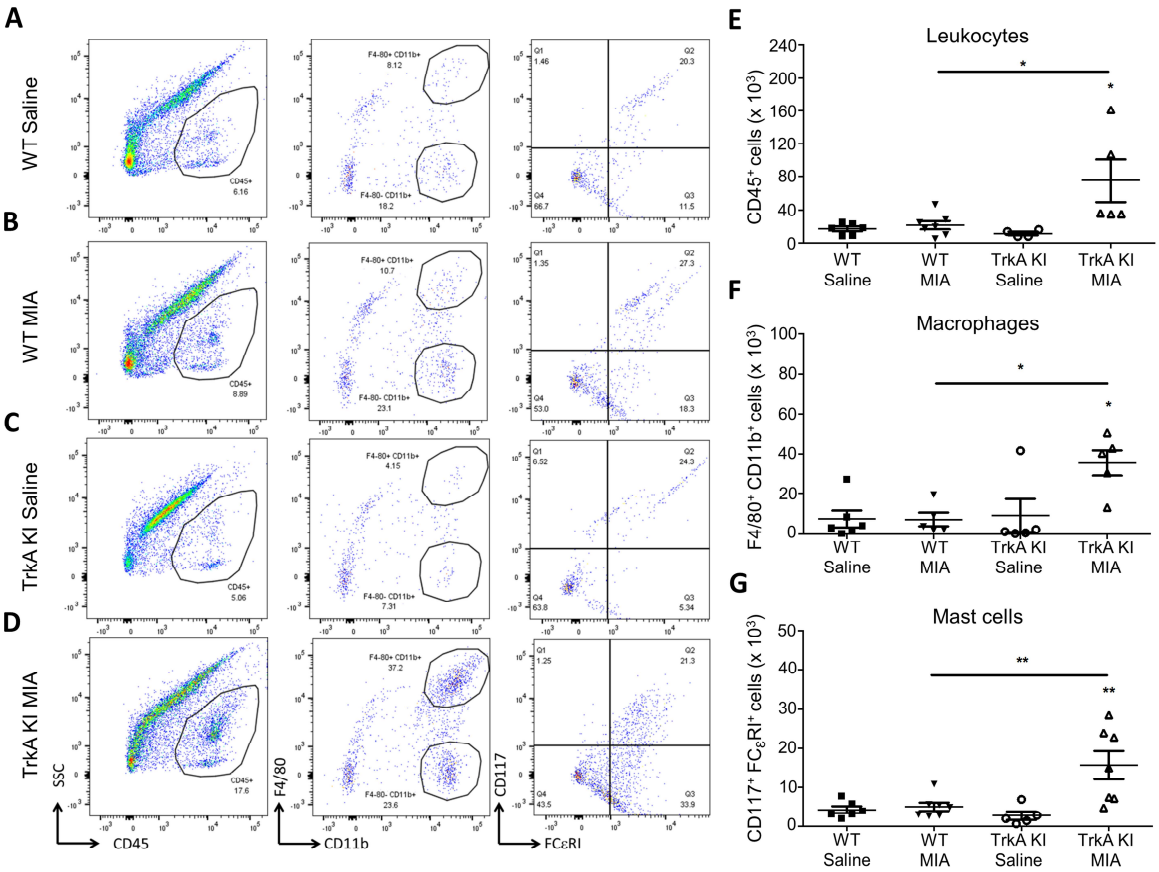
A
WT Saline
B
WT MIA
C
TrkA KI Saline
D
TrkA KI MIA
SSC
CD45
F4/80
CD11b
CD117
FCεRI
E
Leukocytes
CD45+ cells (x 10³)
F
Macrophages
F4/80+ CD11b+ cells (x 10³)
G
Mast cells
CD117+ FCεRI+ cells (x 10³)
WT Saline
WT MIA
TrkA KI Saline
TrkA KI MIA

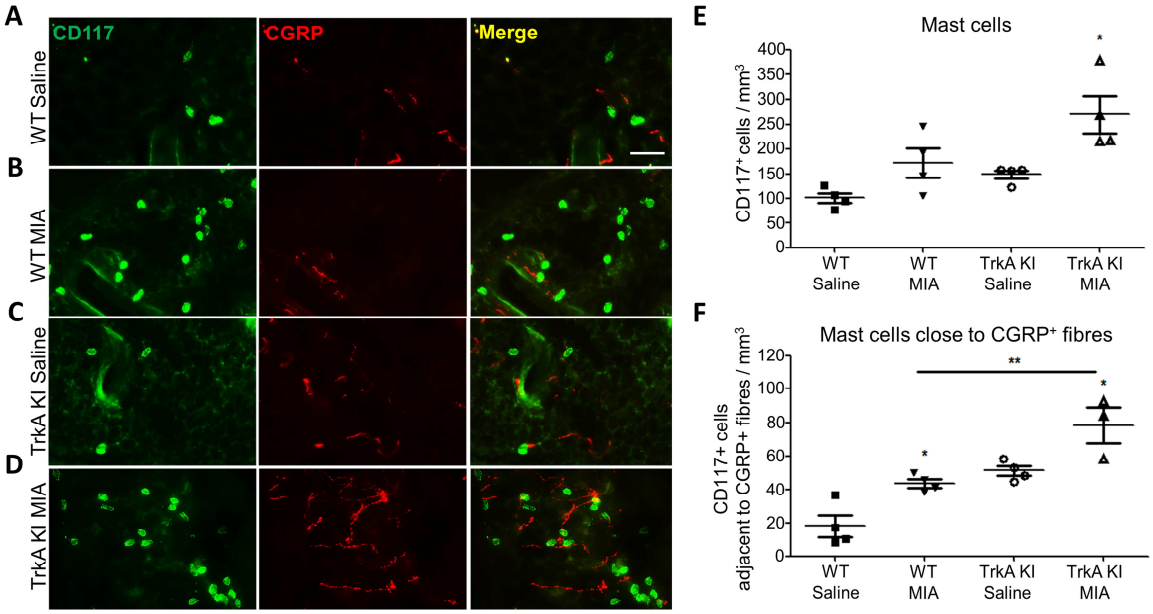
A
B
C
D
CD117
CGRP
Merge
WT Saline
WT MIA
TrkA KI Saline
TrkA KI MIA
E
Mast cells
CD117+ cells / mm3
400
350
300
250
200
150
100
50
0
WT Saline
WT MIA
TrkA KI Saline
TrkA KI MIA
F
Mast cells close to CGRP+ fibres
CD117+ cells adjacent to CGRP+ fibres / mm3
120
100
80
60
40
20
0
**
*
WT Saline
WT MIA
TrkA KI Saline
TrkA KI MIA

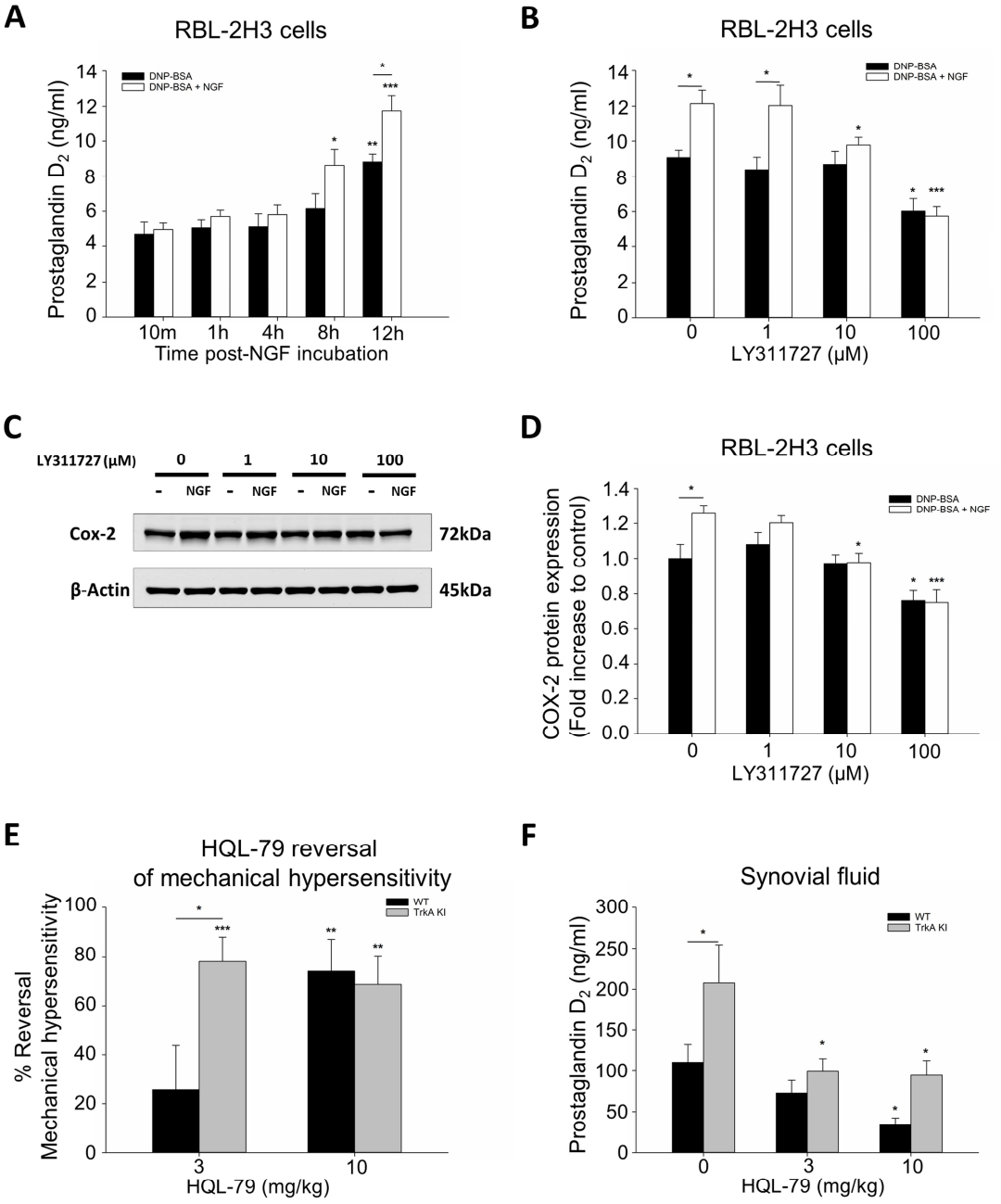
A
RBL-2H3 cells
DNP-BSA
DNP-BSA + NGF
Prostaglandin D2 (ng/ml)
10m
1h
4h
8h
12h
Time post-NGF incubation
B
RBL-2H3 cells
DNP-BSA
DNP-BSA + NGF
Prostaglandin D2 (ng/ml)
LY311727 (μM)
C
LY311727 (μM)
0
1
10
100
NGF
Cox-2
72kDa
β-Actin
45kDa
D
RBL-2H3 cells
DNP-BSA
DNP-BSA + NGF
COX-2 protein expression
(Fold increase to control)
LY311727 (μM)
E
HQL-79 reversal
of mechanical hypersensitivity
WT
TrkA KI
% Reversal
Mechanical hypersensitivity
HQL-79 (mg/kg)
F
Synovial fluid
WT
TrkA KI
Prostaglandin D2 (ng/ml)
HQL-79 (mg/kg)

PAIN

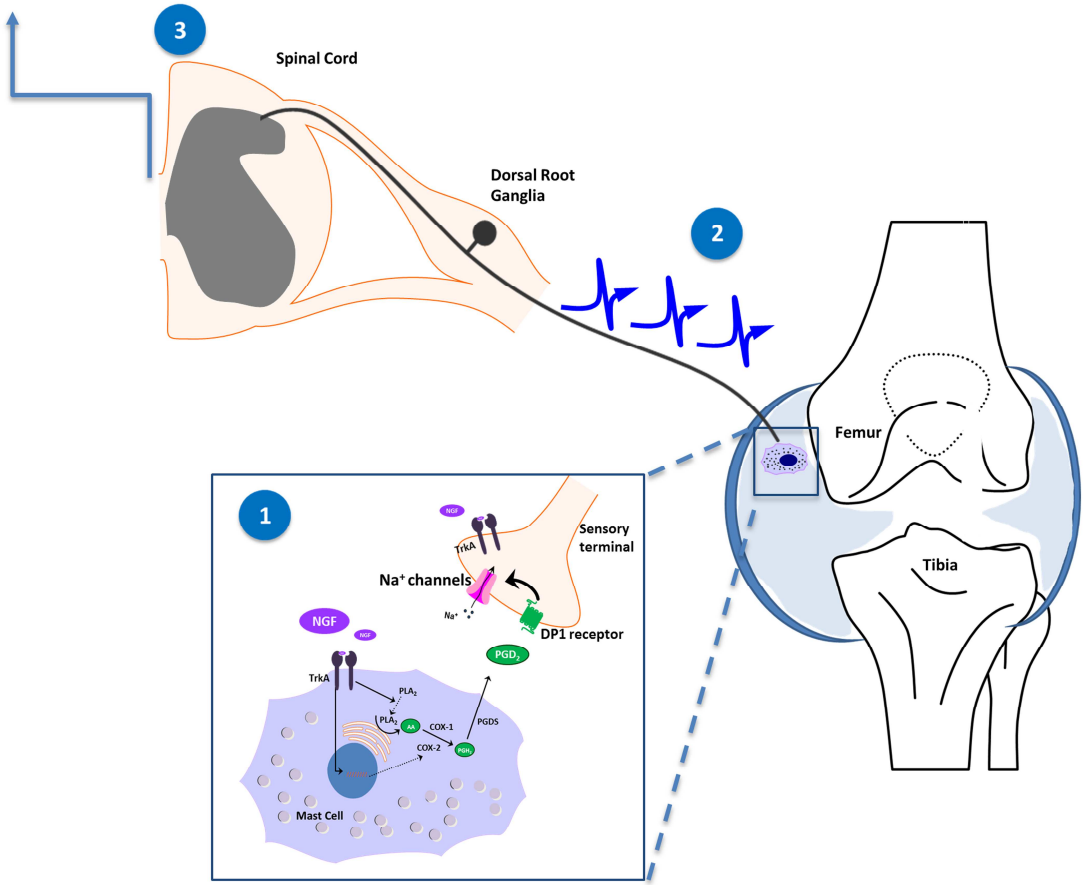
3
Spinal Cord
Dorsal Root
Ganglia
2
Femur
Tibia
1
Sensory
terminal
Na+ channels
DP1 receptor
NGF
TrkA
PGD2
PLA2
AA
COX-1
COX-2
PGDS
Mast Cell